



# The Open Fuels & Energy Science Journal

Content list available at: [www.benthamopen.com/TOEFJ/](http://www.benthamopen.com/TOEFJ/)

DOI: 10.2174/1876973X01609010126



## RESEARCH ARTICLE

# Characterization of a Polymeric Membrane for the Separation of Hydrogen in a Mixture with CO<sub>2</sub>

Dionisio H. Malagón-Romero<sup>1,\*</sup>, Alexander Ladino<sup>2</sup>, Nataly Ortiz<sup>1</sup> and Liliana P. Green<sup>1</sup><sup>1</sup>*Semillero de Energía y Termofluidos, GEAMEC Research Group, Universidad Santo Tomas, Bogotá D.C., Colombia*<sup>2</sup>*Research Group of Fatigue and Surfaces, Universidad del Valle, Cali, Colombia*

Received: July 05, 2016

Revised: November 09, 2016

Accepted: November 09, 2016

**Abstract:** Hydrogen is expected to play an important role as a clean, reliable and renewable energy source. A key challenge is the production of hydrogen in an economically and environmentally sustainable way on an industrial scale. One promising method of hydrogen production is *via* biological processes using agricultural resources, where the hydrogen is found to be mixed with other gases, such as carbon dioxide. Thus, to separate hydrogen from the mixture, it is challenging to implement and evaluate a simple, low cost, reliable and efficient separation process. So, the aim of this work was to develop a polymeric membrane for hydrogen separation. The developed membranes were made of polysulfone *via* phase inversion by a controlled evaporation method with 5 wt % and 10 wt % of polysulfone resulting in thicknesses of 132 and 239 micrometers, respectively. Membrane characterization was performed using scanning electron microscopy (SEM), differential scanning calorimetry (DSC), atomic force microscopy (AFM), and ASTM D882 tensile test. Performance was characterized using a 2<sup>3</sup> factorial experiment using the time lag method, comparing the results with those from gas chromatography (GC). As a result, developed membranes exhibited dense microstructures, low values of RMS roughness, and glass transition temperatures of approximately 191.75 °C and 190.43 °C for the 5 wt % and 10 wt % membranes, respectively. Performance results for the given membranes showed a hydrogen selectivity of 8.20 for an evaluated gas mixture 54% hydrogen and 46% carbon dioxide. According to selectivity achieved, H<sub>2</sub> separation from carbon dioxide is feasible with possibilities of scalability. These results are important for consolidating hydrogen production from biological processes.

**Keywords:** Hydrogen separation, Phase inversion precipitation, Polymeric membranes, Biofuels, Renewable energy, Biohydrogen.

## 1. INTRODUCTION

To ensure energy sustainability in the long term, several scientific and industrial communities worldwide have been researching new energy possibilities with the aim of developing new, efficient, economical, and sustainable energy conversion processes. Among the different candidates, one of the most promising is the hydrogen which is an energy carrier, which has a heating value about 2.75 times greater than that of liquid hydrocarbon fuels gravimetrically, with only water vapor as the combustion product.

The key issue in using hydrogen is associated with production and storage costs [1]. In fact, current production methods have low efficiencies and are not economically feasible in satisfying the current and future needs of hydrogen-based energy as a substitute for fossil fuels [2]. At present, hydrogen represents a market of nearly US\$ 50 billion with a 40 Mt annual production [2], showing a growth rate of approximately 10% per year [3]. Due to these factors involved in energy production, research focused on hydrogen production is important to reduce the costs and obtain more efficient processes. Hydrogen has been traditionally produced *via* chemical processes, such as non-catalytic partial oxidation of fuels, hydrocarbon reforming with steam water, selective oxidation of methane and oxidative dehydration and electrochemical processes [2, 4]. However, in the last few years, hydrogen production has been focused on biological

\* Address correspondence to this author at the Semillero de Energía y Termofluidos, GEAMEC Research Group, Universidad Santo Tomas Cr 9 No 51-11, Bogotá D.C., Colombia; Tel: 57-3012026284; E-mail: [dionisiomalagon@usantotomas.edu.co](mailto:dionisiomalagon@usantotomas.edu.co)

processes [2, 5, 6], where the main principle is to decompose organic molecules into hydrogen and other sub-products during different metabolic cycles. In fact, biological processes for hydrogen production are promising techniques because they offer low production costs and better energy gains compared with chemical-based processes. Additionally, organic residuals and waste water can be used as raw materials [1, 3, 7].

The biological processes for hydrogen production include direct and indirect bio-photolysis, reaction of gaseous interchanging, dark fermentation and photo-fermentation [2]. However, to produce pure hydrogen from these processes, H<sub>2</sub> needs to be separated from a gas mixture (bio-gas) and to reach a concentration as high as 99.99% required by operational standards [8]. The current methods for separating H<sub>2</sub> from other gases (such as CO<sub>2</sub>) are mainly pressure swing adsorption (PSA), cryogenic distillation and adsorption with either amines or aqueous solutions of calcium carbonate [9] and ionic liquids as absorbents with high selectivity capacity for CO<sub>2</sub> separation from other gases [10]. In general, these methods have the disadvantages of high-energy consumptions and high costs.

As a result, separation based on membrane technology has received attention due to its low cost of installation and maintenance, low energy consumption, and advantages in installation, operation and control [11]. In particular, hydrogen separation has been one of the primary applications of polymeric membranes, especially in water-gas shift reactors producing H<sub>2</sub> and CO<sub>2</sub> [8]. Therefore, hydrogen separation using membrane technology can be a promising technique as an efficient and low cost process for hydrogen production, particularly for the energy sector.

One of most employed polymers in membrane fabrication for hydrogen separation is polysulfone, which is an amorphous thermoplastic and has chemical affinity with hydrogen. It also exhibits high chemical resistance to salts and solutions, good fouling resistance and thermal/mechanical integrity mainly due to the aromatic rings in its chemical structure [8, 12 - 15]. Additionally, polysulfone is soluble in different organic solvents, such as dichloromethane and chloroform.

This work focuses on the manufacturing of membranes made by the phase inversion method by controlled evaporation using polysulfone as the polymer and chloroform as the solvent [16, 17]. In this method, the polymer (polysulfone) is dissolved using an organic solvent (chloroform), and the solution is poured into a mold. During the evaporation process of the solvent, a mixture of two phases (solid and liquid) is created, and when evaporation has completed, a membrane is obtained [18]. This method can be used to produce both porous and dense membranes and is the most versatile method to obtain films with different morphological properties depending on the requirements and the particular applications [18]. Another goal of this work is to characterize and test these polymeric membranes, particularly evaluating their performances in the separation of hydrogen from a carbon dioxide/hydrogen mixture.

## 2. MATERIALS AND METHODS

### Chemicals

Polysulfone (Sigma-Aldrich, Mn 22000, Saint Louis, USA) was selected because it is one of the most used materials in fabricating dense membranes for the separation of different gases according to Refs [13 - 15]; Chloroform (Panreac, Barcelona, España) was chosen as the solvent due to its chemical affinity with polysulfone.

### Gas Mixture

To evaluate the separation performance of each fabricated membrane, a gas mixture of 54% hydrogen and 46% carbon dioxide (each with 99.99% purity) was employed. A local distributor of analytical gases (Linde, Bogotá, Colombia) prepared the mixture.

### Methodology for Fabrication of Dense Polymeric Membranes

The fabrication procedure used in this work was based on previous reports [16, 17]. Polysulfone was dissolved in chloroform at 5% wt and 10% wt. A solution of the polymer in chloroform was poured onto petri dishes. Molds were covered using holed aluminum foil and were subjected to controlled evaporation in a chamber furnace (Thermo Scientific, Heraeus Series 6000, West Palm Beach, USA) at 20 °C for 24 hours. Finally, membranes are punched at the size of the permeability cell (50 mm diameter).

### Thickness Measurement

Membrane thicknesses were measured using a dial thickness Gage (Mitotuyo, Kanagawa, Japan). For each

membrane, ten repetitions were made at different points along the membrane. Average values and standard deviations were obtained.

### Tensile Test

Tensile stress tests based on ASTM D882 were developed. Five probes with an area of 32 cm x 3 cm for the 5% wt and 10% wt membranes were mounted in a Universal Testing Machine Shimadzu-UH-50 A (Shimadzu, Kyoto, Japan), with a load of 5 tnf and a displacement velocity of 1 mm s<sup>-1</sup>.

### Scanning Electronic Microscopy (SEM)

Membranes (5 wt % and 10 wt %) were covered with a gold layer in a Denton Vacuum LLC desk IV equipment (Moorestown, USA). SEM was conducted in a JEOL JSM-6490 LV (Peabody, USA) with a voltage of 20 kV.

### Differential Scanning Calorimetry (DSC)

DSC study was performed with a DSC 2910 modulated equipment (TA Instruments, Delaware, USA). A heating ramp of 10 °C min<sup>-1</sup> was utilized between -10 °C to 260 °C.

### Atomic Force Microscopy (AFM)

AFM was used to analyze the surfaces of the membranes. An Atomic Force Microscope MFP3D-BIO (Asylum Research, Santa Bárbara, USA) was employed to determine the membrane roughness in an area of 5 µm x 5 µm.

### Gas Separation Apparatus

For determining selectivity and permeability parameters, a separation apparatus was designed and manufactured, as shown in Fig. (1). The permeability cell is composed of two stainless steel 304 cylindrical chambers. Each chamber has a diameter of 90 mm and a wall thickness of 8 mm, with two ¼ in NPT couplings for the gas inlet and outlet connections. One of the chambers is the support for the membrane. A viton joint and six equally spaced bolts provide the seal in the system. The high and low pressure chambers are separated by the polymeric membrane. On the high-pressure side, the gas mixture is connected to a pressure regulator (V1), which controls the pressure according to the experimental design. Pressure gauges are located at both sides of the membrane. Additionally, a third valve (V3) is located for vacuum generation and purge on the low pressure side of the equipment. Finally, to control the temperature during the test, the entire apparatus is submerged in a thermostatic bath.

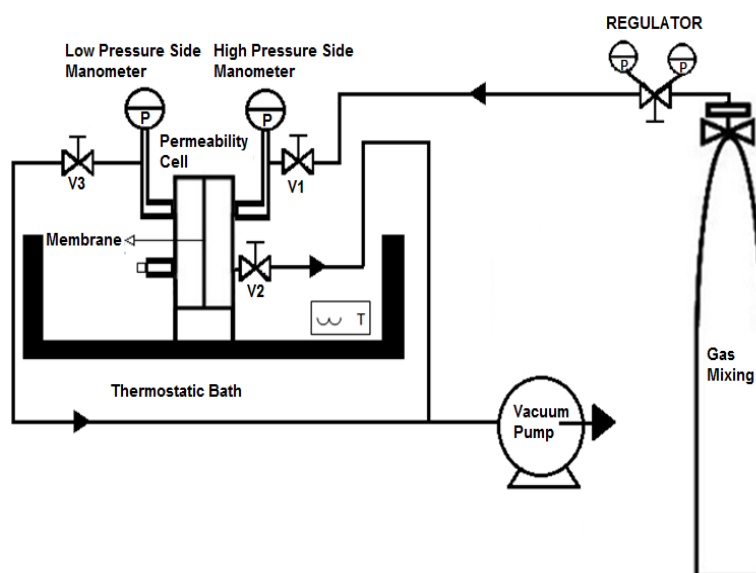


Fig. (1). Schematic view of the equipment used in the separation test.

### 3. MEMBRANE SELECTIVITY AND PERMEABILITY MEASUREMENTS

#### Time Lag Method

The time lag method was used to obtain the individual permeability and selectivity index for both hydrogen (H<sub>2</sub>) and carbon dioxide (CO<sub>2</sub>). In the experiment, membranes were placed in the permeability cell. Afterwards, any gas inside the chambers is evacuated by vacuum for 4 hours. The test starts at time zero (t=0) when valve 1 (V1) is opened, and the membrane is exposed to the gas at the high pressure side. Starting at this time, the pressure on the low-pressure side is monitored [18]. Based on the pressure measurement on the low pressure side, the permeability coefficient (P) is determined according to Equation 1 [19, 20]:

$$P = \frac{273}{76} \left[ \frac{V_b l}{AT p_a} \right] \frac{dp_b}{dt} \quad (1)$$

Where  $P$  is the permeability index (barrers);  $V_b$  is the volume of the low pressure chamber (cm<sup>3</sup>);  $l$  is the membrane thickness (cm);  $A$  is the effective membrane area (cm<sup>2</sup>);  $p_a$  is the gas pressure in the high pressure chamber (cm Hg);  $T$  is the gas temperature (K), and  $dp_b/dt$  is the rate of change of pressure on the low pressure side measured in the linear part of the pressure – time curve (cmHg s<sup>-1</sup>)

The time-lag ( $\theta$ ) is determined by the intersection of the extrapolated pressure – time curve with the x-axis. The time-lag constant enables the calculation of the diffusivity ( $D$ ) according to Equation 2 [21]:

$$D = \frac{l^2}{6\theta} \quad (2)$$

Where  $l$  is the membrane thickness (cm), and  $\theta$  is the time-lag s.

In addition, the selectivity index  $\alpha_{AB}$  was computed. This index can be defined as the capability of a membrane to separate a particular gas A (*i.e.*, hydrogen) from another gas B (*i.e.*, carbon dioxide). This index is the ratio of the permeability of each individual gas to be separated ( $P_A$ ,  $P_B$ ), measured under similar conditions [22]:

$$\alpha_{AB} = \left( \frac{P_A}{P_B} \right) \quad (3)$$

Finally, the solubility coefficient ( $S$ ) is calculated from the diffusivity ( $D$ ) and permeability ( $P$ ) indices according to:

$$S = \frac{P}{D} \quad (4)$$

#### Gas Chromatography (GC) Method

In contrast to the time–lag method, a gas chromatography method was used to determine the composition of the gas that has crossed the membrane. The chromatograph was a Varian 3400 with a Packed Porapak Q (80/10) column and a TCD detector; the carrier gas was nitrogen, column temperature was 70 °C, detector temperature was 180 °C, nitrogen flow was 30 ml min<sup>-1</sup>, injector temperature was 100 °C, filament temperature was 200 °C, and the test time was 6 minutes.

The selectivity index  $\alpha_{AB}$ , based on the gas composition, was computed according to Equation 5:

$$\alpha_{AB} = \frac{y_A/y_B}{x_A/x_B} \quad (5)$$

Where  $y_i$  is the molar fraction of the compound  $i$  in the gas mixture collected on the low pressure side, and  $x_i$  is the molar fraction of the compound  $i$  on the high pressure side of the membrane. A is hydrogen, and B is carbon dioxide.

#### Experimental Design

For the time lag and GC methods, a factorial experiment of 2<sup>3</sup> was developed. The variables examined were operation temperature (25 °C and 35 °C), high pressure side value (3 bar and 4 bar) and polysulfone concentration (5%

wt and 10% wt). The summary of the experimental design is presented in Table 1.

**Table 1. Experimental design used for the evaluation of polysulfone membranes.**

Assay	Temperature °C	Pressure bar	Polysulfone concentration % wt
A	25	3	10
B	25	4	10
C	35	3	10
D	35	4	10
E	25	3	5
F	25	4	5
G	35	3	5
H	35	4	5

## 4. RESULTS

### Characterization of Membranes

The membrane thicknesses were determined to be  $0.132 \pm 0.02$  mm and  $0.289 \pm 0.04$  mm for 5% wt and 10% wt of polysulfone, respectively. Tensile test results are summarized in Table 2.

**Table 2. Tensile test results for 5% wt and 10% wt membranes.**

Percentage of polymer	Ultimate Load N	Ultimate Stress MPa	Maximum Deformation	% strain
5 wt %	$215.75 \pm 50.00$	$38.24 \pm 12.28$	$6.36 \pm 1.15$	$2.12 \pm 0.38$
10 wt %	$476.60 \pm 91.10$	$42.86 \pm 4.48$	$5.02 \pm 2.56$	$1.67 \pm 0.85$

### Differential Scanning Calorimetry (DSC)

DSC curves for 5% wt and 10% wt of polysulfone are presented in Fig. (2). The glass transition temperatures ( $T_g$ ) for the 5% wt and 10% wt membranes were  $191.75^\circ\text{C}$  and  $190.43^\circ\text{C}$ , respectively.

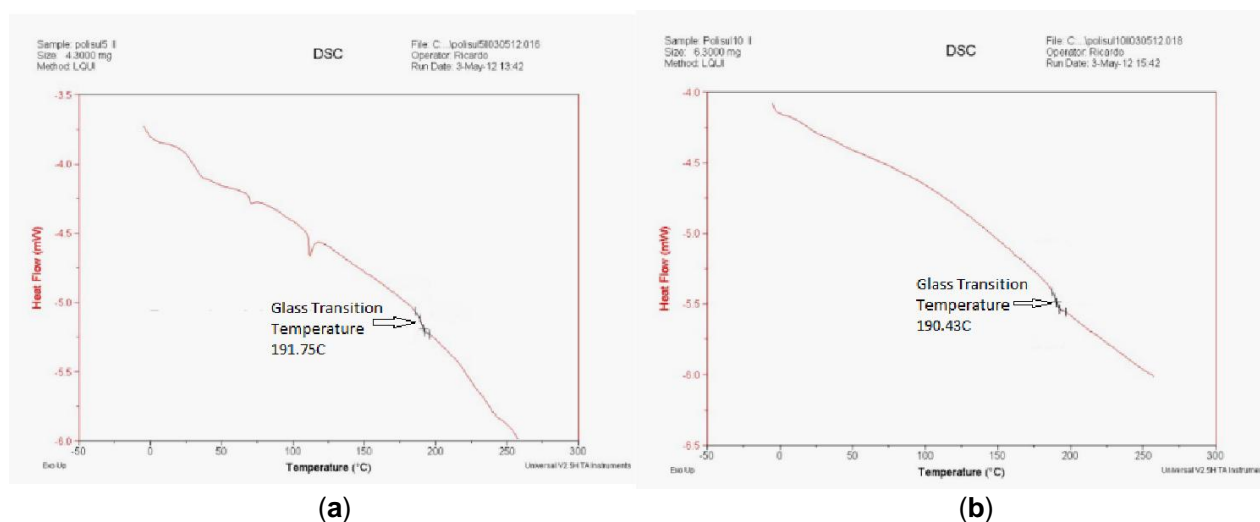


**Fig. (2).** DSC curves for (a) 5% wt and (b) 10% wt membranes.

### Scanning electronic microscopy (SEM) and atomic force microscopy (AFM)

SEM and AFM results are presented in Figs. (3 and 4), respectively. In Fig. (3), SEM results indicate that there is no evidence of pore formation or nucleation, which is important to obtain a suitable microstructure for gas separation.

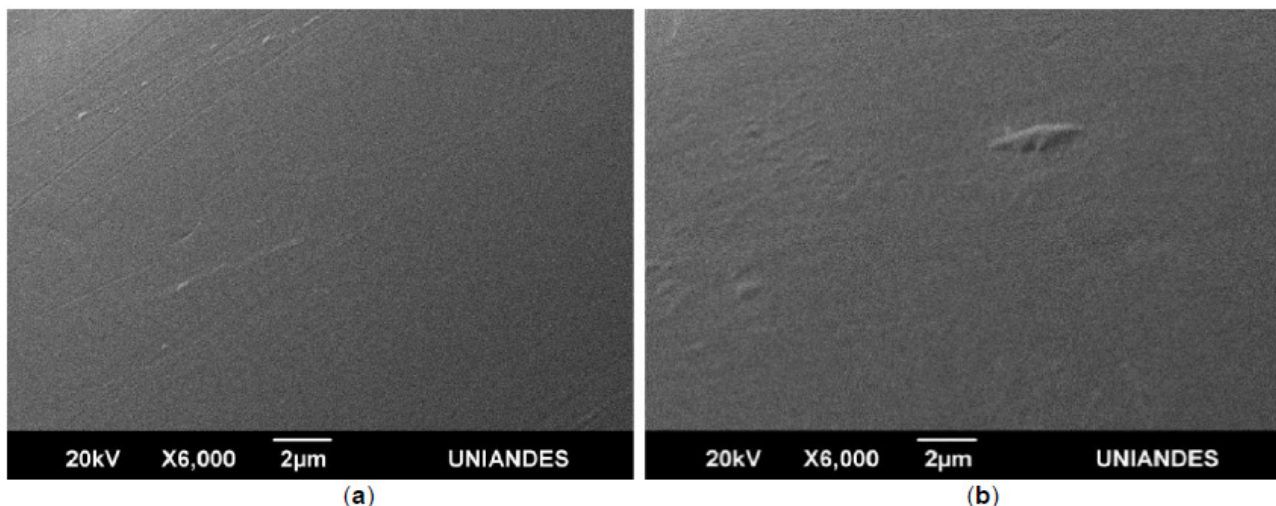


Fig. (3). SEM images of a) 5% wt and b) 10% wt membranes.

Fig. (4) shows the root mean square (RMS) of the surface roughness of the membranes, which are  $2.59 \pm 0.288$  nm and  $6.26 \pm 2.69$  nm for 5 wt % and 10 wt %, respectively. According to these values, 5 wt % of polysulfone concentration leads to a smoother membrane surface.

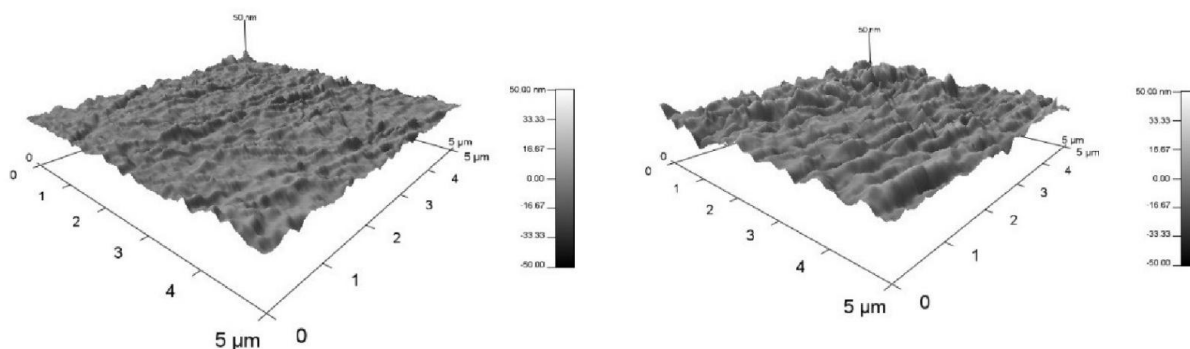


Fig. (4). AFM plot of 5 wt % and 10 wt % membranes (scale of  $5 \mu\text{m} \times 5 \mu\text{m}$ ).

**Time Lag Results**

Based on the time lag method, permeability (P), diffusivity (D) and solubility coefficients (S) were computed for each test for pure hydrogen and carbon dioxide, according to the experimental design presented in Table 1. Afterwards using Equation 3, the selectivity index ( $\alpha_{AB}$ ) was determined. The results are presented in Table 3.

**Table 3. Permeability, diffusivity and solubility for hydrogen and carbon dioxide from the time lag method.**

Assay	Hydrogen			Carbon dioxide			Selectivity (PH <sub>2</sub> /PCO <sub>2</sub> )
	Permeability (barrers)	Diffusivity (cm <sup>2</sup> /s X) E-07	Solubility (cm <sup>3</sup> (STP)/cm <sup>3</sup> cm Hg)	Permeability (barrers)	Diffusivity (cm <sup>2</sup> /s X) E-08	Solubility (cm <sup>3</sup> (STP)/cm <sup>3</sup> cm Hg)	
A	7.43 ± 0.00	4.38 ± 0.36	0.0017	2.97 ± 0.00	4.10 ± 0.25	0.0072	2.50
B	6.69 ± 0.00	4.00 ± 0.40	0.0017	3.34 ± 0.00	4.93 ± 0.06	0.0068	2.00
C	10.07 ± 0.00	4.97 ± 0.47	0.0020	2.88 ± 0.00	5.16 ± 0.27	0.0056	3.50
D	8.092 ± 0.76	8.62 ± 0.94	0.0009	3.24 ± 0.00	9.77 ± 0.42	0.0033	2.50
E	5.09 ± 0.48	1.31 ± 0.10	0.0039	2.72 ± 0.00	1.97 ± 0.14	0.0138	1.87
F	5.86 ± 0.36	1.34 ± 0.16	0.0044	2.80 ± 0.36	2.98 ± 0.11	0.0094	2.09
G	10.51 ± 0.00	2.35 ± 0.32	0.0045	3.94 ± 0.00	3.47 ± 0.22	0.0113	2.66
H	6.41 ± 0.00	2.11 ± 0.00	0.0030	2.71 ± 0.35	2.58 ± 0.08	0.0105	2.36

## Gas Chromatography Results

From the time lag method, the ideal selectivity can be obtained using Equation 4. However, the membrane selectivity has a different behavior when a gas mixture passes across the membrane compared to the case of a pure gas. The molar fraction and selectivity ( $\alpha_{AB}$ ) for each different test combination measured *via* gas chromatography are presented in Table 4. The retention times for hydrogen and CO<sub>2</sub> were  $0.7408 \pm 0.007$  minutes and  $1.6394 \pm 0.016$  minutes, respectively.

**Table 4. Real selectivity values obtained by the GC method.**

Gas Analyzed	Test	Molar Fractions	Selectivity
H <sub>2</sub>	A	0.9058	8.20
CO <sub>2</sub>		0.0941	
H <sub>2</sub>	B	0.8744	5.93
CO <sub>2</sub>		0.1255	
H <sub>2</sub>	C	0.7752	2.94
CO <sub>2</sub>		0.2247	
H <sub>2</sub>	D	0.7663	2.79
CO <sub>2</sub>		0.2336	
H <sub>2</sub>	E	0.8959	7.34
CO <sub>2</sub>		0.1040	
H <sub>2</sub>	F	0.8529	4.94
CO <sub>2</sub>		0.1470	
H <sub>2</sub>	G	0.7900	3.21
CO <sub>2</sub>		0.2099	
H <sub>2</sub>	H	0.6950	1.94
CO <sub>2</sub>		0.3049	

## 5. ANALYSIS OF RESULTS

### Membrane Manufacturing

As shown in Table 2, the 10% wt membrane exhibits a greater ultimate tensile strength (UTS) and lower strain than the 5% wt membrane. Hence, the concentration of polymer is a factor that can increase the strength and stiffness of the membrane. It is obvious that if the polymer concentration increases, the thickness and stiffness also increase according to the fabrication method employed. This behavior is observed because the membrane made from a lower polymer concentration has a greater mobility between the polymeric chains, resulting in a more flexible and deformable membrane than the one made from a higher polymer concentration. Additionally, DSC results show that the polysulfone concentration does not affect the glass transition temperature.

On the other hand, RMS roughness measurements show that a smoother surface is achieved in the membrane made from 5% wt of polysulfone. This behavior can be explained by the fact that the molecules have more time and space to reorganize in a uniform way. Additionally, in contrast to the results reported by Batina *et al.* [23], the roughness values obtained for both membranes in this study are smaller, indicating the membranes are smoother. It is worth noting that according to Macanás [24], transport properties should not be affected by small irregularities on the membrane surface. Finally, the surface does not show evidence of porosity for both polymer concentrations, indicating that both membranes are dense.

### Time Lag Results

A variation analysis (Design Expert V. 8.0.4.1) for the obtained results was developed and presented in the Table 5, where the percentage of influence (effect) of each independent variable over the dependent variables is evaluated.

Table 5. Variation analysis.

Source	Percentage contribution							
	Diffusivity CO <sub>2</sub>	Diffusivity H <sub>2</sub>	Permeability CO <sub>2</sub>	Permeability H <sub>2</sub>	Solubility CO <sub>2</sub>	Solubility H <sub>2</sub>	Selectivity time lag	Selectivity GC method
Temperature: A	14.67	14.36	8.74	47.39	6.81	5.56	44.85	80.78
Pressure: B	9.19	2.18	1.75	17.27	9.95	10.41	17.09	12.32
Polymer concentration: C	50.11	69.45	0.66	9.12	75.36	58.98	15.81	1.96
AB	1.06	3.50	17.82	17.50	0.43	16.77	7.12	3.52
AC	6.89	2.76	18.15	1.92	2.12	2.57	1.33	0.55
BC	8.45	2.88	35.64	0.24	1.01	1.32	13.80	0.53
ABC	9.64	4.88	17.24	6.57	4.32	4.39	0.00	0.34

In this analysis, the effect of the three independent variables (temperature, pressure and polymer concentration) over diffusivity (D), permeability (P), solubility (S) and selectivity ( ) was studied. According to the results obtained in this study, H<sub>2</sub> permeability is mainly a function of temperature (percentage of influence is 47.39%), while CO<sub>2</sub> permeability is more influenced by the combined interactions of pressure and polymer concentration (35.64%). Regarding diffusivity, the polymer concentration is the most influential factor for both H<sub>2</sub> (69.45%) and CO<sub>2</sub> (50.11%). Finally, the solubility is affected mainly by the polymer concentration for both H<sub>2</sub> (58.98%) and CO<sub>2</sub> (75.36%).

In the case of temperature effects, when the temperature rises, the gas molecules have more kinetic energies, which enhance the molecular transport across the membrane. In addition, a temperature increment in the whole system, and consequently in the membrane, enhances the mobility of the polymeric chains and improves the gas motion across the membrane. Moreover, since the kinetic diameter of H<sub>2</sub> is less than carbon dioxide, hydrogen can move more easily across the polymeric matrix, which improves the diffusion process for H<sub>2</sub>, as can be observed in Table 3. In summary, a temperature rise increases diffusivity (D) and permeability (P) and reduces solubility (S) for both H<sub>2</sub> and CO<sub>2</sub>. These results are in agreement with previous studies, such as the work of Naddakati *et al.* [25].

In addition, a pressure increment generates a reduction in H<sub>2</sub> permeability. This effect can be due to the level of H<sub>2</sub> absorption inside the polymer matrix, which is enhanced due to the low kinetic diameter of H<sub>2</sub> and the pressure rise. This behavior may be due to the absorption of hydrogen into the polymeric network, which is also favorable due to its low kinetic diameter. This observed phenomenon is in contrast with that reported in Ref [26], in which the permeability of the gases, such as hydrogen, remained almost constant when the gases were between 2 bar and 10 bar. Finally, the solubility (S) remains constant and is independent of pressure changes, in contrast to the diffusivity (D), which increases with pressure.

In contrast to the pressure effect on H<sub>2</sub> behavior as reported by Bos [27], a greater pressure on the high-pressure side induces a greater number of CO<sub>2</sub> molecules to interact with the polymeric matrix, resulting in polymer plasticization. This reveals that the permeability and diffusivity coefficients grow with pressure, while solubility is reduced. A reduction in the gas permeability for CO<sub>2</sub> is associated with a decrease in the gas solubility coefficient (S) with pressure. This phenomenon occurs because the polymer sorption sites become saturated with gas molecules at increasing values of pressure. When plasticization occurs, the polymeric chains are disrupted by the gas molecules that enable diffusion (D), which therefore increases the permeability (P) [26].

Moreover, an increment in the polymer concentration leads to an increase in the thickness of the membrane under the same fabrication conditions and procedures. However, the membrane thickness, which enhances the mechanical performance, produces a drop in the diffusion coefficient (D). This is because molecules have to travel a greater distance across the polymeric matrix. In a similar way, the solubility is reduced with membrane thickness, but the permeability coefficient rises.

Finally, the selectivity, which is defined as the ratio between H<sub>2</sub> and CO<sub>2</sub> permeabilities, is greater than 1. This indicates that separation is achieved for both gases. The main factor that affects the selectivity ( Table 5) is: temperature (44.85%), followed by pressure (17.09%) and polymer concentration (15.81%). As a matter of fact, selectivity rises with temperature because it is proportional to diffusivity. Additionally, selectivity is improved with increasing membrane thickness, due to the increase of permeability of both gases. Since all permeability test results show that the H<sub>2</sub> permeability is greater than the CO<sub>2</sub> permeability, it can be concluded that hydrogen separation *via* the polymeric

membrane is feasible. The best results are for the C test case (*i.e.*, 35 °C, 3 bar and 10% w.t polymer concentration).

### Gas Chromatography Results

Membrane selectivity determined *via* gas chromatography is considered as the actual selectivity. This is because the analysis implicitly involves the real interaction between both gases, in contrast to the time lag method where the selectivity is determined for each gas separately. In fact, the GC method directly analyzes the composition of the gas that has crossed the polymer membrane.

According to the obtained results shown in Table 5, selectivity is mainly affected by temperature (80.72%) in an inverse manner, *i.e.*, when the temperature is increased, the selectivity is reduced, and separation is improved at 25 °C compared with the same conditions at 35 °C. In contrast, the polymer concentration and pressure have low effects (1.96% and 12.32%, respectively) on selectivity, where the concentration and pressure are directly and inversely correlated to the selectivity, respectively. The best conditions according to the chromatograph results correspond to test case A (25 °C, 10% w.t polymer concentration and 3 bar).

In both methods, the temperature is found to be the main factor that influences selectivity. Additionally, in both methods, the selectivity is inversely correlated with the temperature; hence, the temperature is chosen to be 25 °C for the separation process. In addition, both methods reveal an inverse relation between the pressure and selectivity and a direct relation between the polymer concentration (membrane thickness) and selectivity.

To conclude, both methods are in agreement on the best conditions for separation, in terms of the pressure (3 bar) and the polymer concentration (10% w.t). However, the two methods show different trends for temperature. For the time-lag method, the best condition is at 35 °C, and for the GC method, the ideal temperature is 25 °C. This discrepancy can be explained by the fact that in the time lag method, only one gas is tested at a time, and when the temperature rises, the kinetic energy of the gas molecules rises, enhancing the diffusion process for molecules with the same kinetic diameters (*i.e.*, pure H<sub>2</sub> or pure CO<sub>2</sub>). However, in the case of a CO<sub>2</sub>-H<sub>2</sub> mixture with several orders of difference between the kinetic diameters of CO<sub>2</sub> and H<sub>2</sub>, hydrogen diffusion becomes more complicated due to its smaller diameter. Because the GC method directly analyzes the probe after the separation process, the best conditions obtained from this work are ones described for test case A.

A comparison of the current results to data from other authors is presented in Table 6 at a temperature of 35 °C. As can be seen, the selectivity obtained by the GC method is on the same order as the values reported by other authors and reveals that an effective separation of hydrogen and carbon dioxide is possible. The main parameter that determines gas separation is the selectivity determined from results given by the GC method. According to the results obtained, the concentration of hydrogen increased from 54% (before the membrane) to 90.58% (after the membrane).

**Table 6. Permeability and selectivity values for (H<sub>2</sub>/CO<sub>2</sub>) mixtures at 35.**

Author	Permeability H <sub>2</sub> (barrers)	Permeability CO <sub>2</sub> (barrers)	Selectivity Time-Lag Method	Selectivity GC Method
Present Work	8.77	3.19	2.75	2.72
Gorgojo [28]	11.8	5.9	N/A	2
Ahn <i>et al.</i> [14]	11.8	6.3	1.87	N/A
Mohr <i>et al.</i> [29]	13.6	6.7	2.03	N/A
McHattie <i>et al.</i> [30]	14	5.6	N/A	2.5

### CONCLUSION

This paper focused on the fabrication and performance evaluation of polymer membranes for hydrogen separation from a CO<sub>2</sub> – H<sub>2</sub> mixture. In this study, the obtained membranes were able to separate a mixture of these gases. This is an advantage because, by using membranes, it is possible to integrate the separation process into hydrogen production in a fermenter. In this scenario, temperatures are close to ambient temperatures compared with other methods of hydrogen production. Furthermore, the method of membrane production proposed in this study is easy, economical, and reproducible. Additionally, it is possible to scale-up to an industrial process. Finally, the best conditions for hydrogen separation were found to be 25 °C and 3 bar using membranes made from 10% wt of polysulfone, and the obtained selectivity was 8.2.

## CONFLICT OF INTEREST

The authors confirm that this article content has no conflict of interest.

## ACKNOWLEDGEMENTS

The present work was sponsored by Universidad Santo Tomas through FODEIN Code: 6013011103.

## REFERENCES

- [1] Chong, M-L.; Sabaratnam, V.; Shirai, Y.; Hassan, M.A. Biohydrogen production from biomass and industrial wastes by dark fermentation. *Int. J. Hydrogen Energy*, **2009**, *34*, 3277-3287. [http://dx.doi.org/10.1016/j.ijhydene.2009.02.010]
- [2] Dincer, I. Green methods for hydrogen production. *Int. J. Hydrogen Energy*, **2012**, *37*(2), 1954-1971. [http://dx.doi.org/10.1016/j.ijhydene.2011.03.173]
- [3] Kapdan, I.K.; Kargi, F. Bio-hydrogen production from waste materials. *Enzyme Microb. Technol.*, **2006**, *38*(5), 569-582. [http://dx.doi.org/10.1016/j.enzmictec.2005.09.015]
- [4] Dolgykh, L.; Stolyarchuk, I.; Deynega, I.; Strizhak, P. The use of industrial dehydrogenation catalysts for hydrogen production from bioethanol. *Int. J. Hydrogen Energy*, **2006**, *31*(11), 1607-1610. [http://dx.doi.org/10.1016/j.ijhydene.2006.06.028]
- [5] Acar, C.; Dincer, I. Comparative assessment of hydrogen production methods from renewable and non-renewable sources. *Int. J. Hydrogen Energy*, **2014**, *39*(1), 1-12. [http://dx.doi.org/10.1016/j.ijhydene.2013.10.060]
- [6] Bernal, M.; Tinoco, L.K.; Torres, L.; Malagón-Romero, D.; Montoya, D. Evaluating Colombian *Clostridium* spp. strains' hydrogen production using glycerol as substrate. *Electron. J. Biotechnol.*, **2013**, *16*(2), 6.
- [7] Han, S-K.; Shin, H.S. Biohydrogen production by anaerobic fermentation of food waste. *Int. J. Hydrogen Energy*, **2004**, *29*(6), 569-577. [http://dx.doi.org/10.1016/j.ijhydene.2003.09.001]
- [8] Shao, L.; Low, B.T.; Chung, T-S.; Greenberg, A.R. Polymeric membranes for the hydrogen economy: Contemporary approaches and prospects for the future. *J. Membr. Sci.*, **2009**, *327*(1-2), 18-31. [http://dx.doi.org/10.1016/j.memsci.2008.11.019]
- [9] Hosseini, S.S.; Teoh, M.M.; Chung, T.S. Hydrogen separation and purification in membranes of miscible polymer blends with interpenetration networks. *Polymer (Guildf.)*, **2008**, *49*(6), 1594-1603. [http://dx.doi.org/10.1016/j.polymer.2008.01.052]
- [10] Völkl, J.; Müller, K.; Mokrushina, L.; Arlt, W. A priori property estimation of physical and reactive CO<sub>2</sub> absorbents. *Chem. Eng. Technol.*, **2012**, *35*(3), 579-583. [http://dx.doi.org/10.1002/ceat.201100319]
- [11] Sanders, D.F.; Smith, Z.P.; Guo, R.; Robeson, L.M.; McGrath, J.E.; Paul, D.R.; Freeman, B.D. Energy-efficient polymeric gas separation membranes for a sustainable future: A review. *Polymer (Guildf.)*, **2013**, *54*(18), 4729-4761. [http://dx.doi.org/10.1016/j.polymer.2013.05.075]
- [12] Rajagopalan, G.; Immordino, K.M.; Jr, J.W.; Mcknight, S.H. Diffusion and reaction of epoxy and amine in polysulfone studied using Fourier transform infrared spectroscopy : experimental results. *Polymer (Guildf.)*, **2000**, *41*, 2591-2602. [http://dx.doi.org/10.1016/S0032-3861(99)00418-8]
- [13] Lee, W-J.; Kim, D-S. Kim, J.-H. Preparation and gas separation properties of asymmetric polysulfone membranes by a dual bath method. *Korean J. Chem. Eng.*, **2000**, *17*(2), 143-148. [http://dx.doi.org/10.1007/BF02707135]
- [14] Ahn, J.; Chung, W-J.; Pinnau, I.; Guiver, M.D. Polysulfone/silica nanoparticle mixed-matrix membranes for gas separation. *J. Membr. Sci.*, **2008**, *314*, 123-133. [http://dx.doi.org/10.1016/j.memsci.2008.01.031]
- [15] Powell, C.E.; Qiao, G.G. Polymeric CO<sub>2</sub>/N<sub>2</sub> gas separation membranes for the capture of carbon dioxide from power plant flue gases. *J. Membr. Sci.*, **2006**, *279*, 1-49. [http://dx.doi.org/10.1016/j.memsci.2005.12.062]
- [16] Torres-Trueba, A.; Ruiz-Treviño, F.A.; Luna-Bárceñas, G.; Ortiz-Estrada, C.H. Formation of integrally skinned asymmetric polysulfone gas separation membranes by supercritical CO<sub>2</sub>. *J. Membr. Sci.*, **2008**, *320*, 431-435. [http://dx.doi.org/10.1016/j.memsci.2008.04.024]
- [17] Reverchon, E.; Cardea, S. Formation of polysulfone membranes by supercritical CO<sub>2</sub>. *J. Supercrit. Fluids*, **2005**, *35*, 140-146. [http://dx.doi.org/10.1016/j.supflu.2004.12.007]
- [18] Young, T-H.; Huang, Y-H.; Chen, L-Y. Effect of solvent evaporation on the formation of asymmetric and symmetric membranes with crystallizable EVAL polymer. *J. Membr. Sci.*, **2000**, *164*(1-2), 111-120. [http://dx.doi.org/10.1016/S0376-7388(99)00210-0]

- [19] Hosseini, S.S.; Peng, N.; Chung, T.S. Gas separation membranes developed through integration of polymer blending and dual-layer hollow fiber spinning process for hydrogen and natural gas enrichments. *J. Membr. Sci.*, **2010**, *349*(1–2), 156-166. [<http://dx.doi.org/10.1016/j.memsci.2009.11.043>]
- [20] Villaluenga, J.P.; Seoane, B. Permeation of carbon dioxide through multiple linear low-density polyethylene<sup>®</sup> lms. *Eur. Polym. J.*, **2000**, *36*, 1697-1702. [[http://dx.doi.org/10.1016/S0014-3057\(99\)00229-3](http://dx.doi.org/10.1016/S0014-3057(99)00229-3)]
- [21] Boes, N.; Züchner, H. Electrochemical methods for studying diffusion, permeation and solubility of hydrogen in metals. *J. Less Common Met.*, **1976**, *49*, 223-240. [[http://dx.doi.org/10.1016/0022-5088\(76\)90037-0](http://dx.doi.org/10.1016/0022-5088(76)90037-0)]
- [22] Yampolskii, Y. Polymeric gas separation membranes. *Macromolecules*, **2012**, *45*, 3298-3311. [<http://dx.doi.org/10.1021/ma300213b>]
- [23] Batina, N.; Acosta García, M.C.; Avalos Pérez, A.; Alberto Ramírez, M.; Franco, M.; Pérez Gravas, H.; Cadena Méndez, M. Structural changes of polysulfone membrane use for hemodialysis in the consecutive regime: nanometric analysis by AFM. *4<sup>th</sup> International Conference on Smart Materials and Nanotechnology in Engineering*, **2013**, 8793, 87931Q-87931Q. [<http://dx.doi.org/10.1117/12.2027844>]
- [24] Macanás, J.; Palacio, L.; Prádanos, P.; Hernández, A.; Muñoz, M. Atomic force microscopy as a suitable technique for surface characterization of activated composite membranes for metal ion facilitated transport. *Appl. Phys., A Mater. Sci. Process.*, **2006**, *84*(3), 277-284. [<http://dx.doi.org/10.1007/s00339-006-3609-x>]
- [25] Nadakatti, S.M.; Kim, J.H.; Stern, S.A. Solubility of light gases in poly (n-butyl methacrylate) at elevated pressures. *J. Membr. Sci.*, **1995**, *108*, 279-291. [[http://dx.doi.org/10.1016/0376-7388\(95\)00182-4](http://dx.doi.org/10.1016/0376-7388(95)00182-4)]
- [26] David, O.; Gorri, D.; Nijmeijer, K. Hydrogen separation from multicomponent gas mixtures containing CO, N<sub>2</sub> and CO<sub>2</sub> using Matrimid<sup>®</sup> asymmetric hollow fiber membranes. *J. Membr.*, **2012**, *419-420*, 49-56. [<http://dx.doi.org/10.1016/j.memsci.2012.06.038>]
- [27] Bos, A.; Punt, I.G.; Wessling, M.; Strathmann, H. CO<sub>2</sub> -induced plasticization phenomena in glassy polymers. *J. Membr. Sci.*, **1999**, *155*, 67-78. [[http://dx.doi.org/10.1016/S0376-7388\(98\)00299-3](http://dx.doi.org/10.1016/S0376-7388(98)00299-3)]
- [28] Gorgojo, P. *Desarrollo de materiales laminares porosos para la preparación de membranas híbridas*; Universidad de Zaragoza, **2010**.
- [29] Mohr, J.M.; Paul, D.R.; Pinnau, I.; Koros, W.J. Surface fluorination of polysulfone asymmetric membranes and films. *J. Membr. Sci.*, **1991**, *56*(1), 77-98. [[http://dx.doi.org/10.1016/0376-7388\(91\)85016-X](http://dx.doi.org/10.1016/0376-7388(91)85016-X)]
- [30] McHattie, J.S.; Koros, W.J.; Paul, D.R. Gas transport properties of polysulphones: 1. Role of symmetry of methyl group placement on bisphenol rings. *Polymer (Guildf.)*, **1991**, *32*(5), 840-850. [[http://dx.doi.org/10.1016/0032-3861\(91\)90508-G](http://dx.doi.org/10.1016/0032-3861(91)90508-G)]